Nuclear Physics B90 (1975) 52–76

FIELD THEORETIC MODEL FOR THE PION FORM FACTOR

F. GUTBROD and U. WEISS*
Deutsches Electronen-Synchrotron DESY, Hamburg, Germany

Received 26 June 1974
(Revised 7 October 1974)

We present the formalism of a field theoretic many-channel model for the electromagnetic form factors of the $\pi\pi$, the $K\bar{K}$ and the $\pi\omega$ system. The main attractive force, which generates the ρ-meson, is derived from the nucleon box diagram with phenomenological strong vertex corrections. Propagator self-energy corrections are derived from the Ward identity. Long range forces are introduced through the pion exchange coupling between the $\pi\pi$ and $\rho\epsilon$ channel. The photon is coupled minimally to pions, kaons and nucleons, with subtractions performed at large spacelike momenta. The model is solved in the framework of the Bethe-Salpeter equation.

Three different versions are considered which lead to slightly different pion form factors. The version giving the best $\pi\pi$ phase agrees best with the data in the space-like region.

1. Introduction

The electromagnetic form factors of elementary particles in the time like region will provide us with much information about strong interaction dynamics. It could be for instance that the pion form factor (f.f.) turns out to be dominated by many resonance poles [1–3] or that it shows, shortly after the ρ-bump, the same smooth power fall off as in the space like region or that it does so, if at all, only beyond e.g. the $N\bar{N}$ threshold. This detailed behaviour will clarify many questions. This is especially true if we do not consider theoretically just one isolated form factor but try to understand, at moderate energies at least, several channels like $\pi\pi$, $\pi\omega$ and $N\bar{N}$ as a strongly coupled system in the spin-1 state. Then all these f.fs. are mutually dependent. The unique possibility to study the production of these states in e^+e^- collisions in a pure spin state makes it worthwhile to devote much effort on theoretical models which incorporate the multichannel aspect. Phenomenological attempts (without detailed "dynamical" assumptions) have been undertaken several times [4–6].

Of course in the energy region** $\sqrt{s} < 2$ GeV the ρ-meson (and possible higher

* On leave of absence from Institut für Theoretische Physik der Universität Stuttgart.
** We denote the photon four-momentum by P and use $P^2 = s = W^2$.

vector mesons) will have a dominant influence on the pion f.f. $F_\pi(s)$. Therefore a reasonable model for the ρ-meson has to be the starting point, and we do not believe that a knowledge of the $\pi\pi$ scattering phase shift alone can substitute this for the following reason. Since there is little hope that the ρ can be described as a predominantly elastic $\pi\pi$ state [7], the use of the Omnès formula [8–10] which is based on analyticity and elastic unitarity, can hardly be justified. It is tempting to describe the ρ-meson as a resonance (or bound state resp.) between more elmentary constituents, and as those we take $\pi\pi$, $K\bar{K}$ and $N\bar{N}$ states*. We shall make the assumption that the dominant forces which these constituents feel, are not usual one-particle exchange forces for the various elastic scattering amplitudes, but are exchange forces which lead from one channel to another ("non-diagonal forces"). It has been pointed out in ref. [11] that when one considers only the $\pi\pi$ and the $N\bar{N}$ channel in the framework of the Bethe-Salpeter equation (BSE), one finds a ρ-meson which is immensely broad. If in addition to the $\pi\pi$ channel one takes into account those states which contribute to the pion self-energy, the situation is improved considerably. These self-energy effects can be determined self-consistently [12] from the Ward identity once the electromagnetic vertex of the pion is calculated off-shell with the help of the BSE. The ρ-width can be reduced further if one couples also the $\pi\omega$ channel to the ρ, mainly because of the special energy dependence of the $\pi\pi \to \pi\omega$ transition amplitude [12].

It remains however impossible to explain a ρ-width of 140 MeV without stretching the strength of the $\pi\omega\rho$ coupling beyond acceptable values. In principle it is not surprising that the restriction to a finite number of channels will cause a too large coupling of the resonance to the channels under consideration, i.e. a too large $\pi\pi$ width. We may simulate the coupling to neglected channels by increasing the dressed pion propagators beyond the value dictated by the Ward identity.

Another possibility of improving our model with respect to the ρ-width is indicated by the use of chiral invariant πN Lagrangians for the calculation of the nucleon

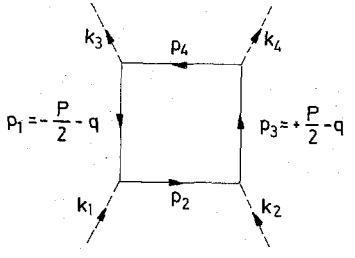

Fig. 1. Nucleon-loop contribution to the $\pi\pi$ Bethe-Salpeter kernel. Propagators and vertices are dressed ones.

* We also shall consider $\pi^0\omega$ and $\rho\epsilon$ states which is reasonable as long as they can be regarded as corrections.

loop [13–15] (we recall from ref. [11] that the nucleon loop of fig. 1 is considered as the main driving force in the $\pi\pi$ channel). These Lagrangians possess quadrilinear couplings, which drastically change the energy behaviour of the loop as compared to the result of standard pseudoscalar coupling. Of course due to divergences one cannot really calculate a resonance with this Lagrangian as a pole in the strong coupling constant*. However, it is plausible that similar modifications in the nucleon loop might arise from pion exchange insertions inside the loop which do not destroy the renormalizability. We shall introduce such changes in the kernel of the BSE for $\pi\pi$ scattering on a phenomenological level. We think that the ρ-width can finally be explained with reasonable modifications.

The non-diagonal forces between the $\pi\pi$, $\pi\omega$ and $N\bar{N}$ channels are of short range nature. Long range forces, which are especially important at energies below the ρ-mass, are introduced into the model by the one-pion exchange force between the $\pi\pi$ and $\rho\epsilon$ force. After one iteration this leads to the box contribution of fig. 2a, and we also included the crossed box diagram of fig. 2b as a force in the $\pi\pi$ channel.

The coupling of the photon to the various channels introduces only few additional problems. We assume that pions, kaons and nucleons act as bare constituents with minimal e.m. couplings, and we have to perform subtractions for their divergent vertex diagrams. The divergences are logarithmic due to a balance of vertex and propagator modifications, which we introduce in the nucleon loop.

In sect. 2 we describe the mentioned modifications of the nucleon loop and the subtraction for the e.m. vertices. In sect. 3 the coupling of the $\pi\omega$ channel to the ρ will be discussed together with the question of normalization of the $\pi\omega\gamma$ vertex. In sect. 4 we present the calculation of the $\rho\epsilon$ loop. Since the $\rho\epsilon$ channel causes great difficulties for solving the BSE equation, we shall discuss the detailed method of numerical solution elsewhere. Thus sect. 5 contains only the numerical results for the $\pi\pi$ phase shift and the pion f.f., which after the inclusion of the $\rho\epsilon$ channel compare favourably with the existing data. The discussion and an outlook follows in sect. 6.

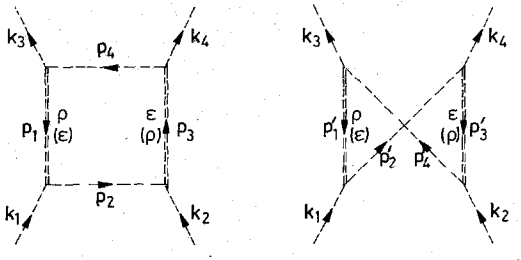

Fig. 2. (a) $\rho\epsilon$ loop contribution to the $\pi\pi$ Bethe-Salpeter kernel. The internal propagators are free ones. (b) Crossed $\rho\epsilon$-loop contribution to the $\pi\pi$ Bethe-Salpeter kernel.

* In the quoted papers the pole is generated by the replacement $1 + g^2 \to 1/(1 - g^2)$.

2. Nucleon loop contributions to the pion form factor

In this section we want to discuss the force in the $\pi\pi$ channel which is responsible for the ρ resonance. As summarized in ref. [16], the direct $\pi\pi$ interaction $L_1 = \lambda : (\pi \cdot \pi)^2 :$ is not a good candidate as far as can be judged from the low order calculations performed so far. Derivative Lagrangians like [13–15] $L_1 = -f_\pi^2 : (\partial_\mu \pi)^2 \pi^2 :$ lead to unbypassed difficulties in higher orders and in the e.m. current, and up to second order do not seem to produce a resonance. Consequently we shall concentrate here on the force provided by the nucleon loop contribution to the $\pi\pi$ irreducible amplitude shown in fig. 1. Repeating the essential results from refs. [11,12], its properties are the following: Calculated in γ_5 theory with $g^2/4\pi = 14.5$, it gives an attractive potential which is too large by more than an order of magnitude to give a ρ-meson at the correct mass. We proposed to weaken the strong interaction by introducing phenomenological hadronic vertex functions which decrease for growing spacelike momenta. However we do not intend to convert the model into a superrenormalizable one, since this would probably lead to finite e.m. form factors at infinite momentum transfer. Therefore we shall work (as it is recommended anyhow) with dressed propagators for pions and nucleons, which compensate the fall-off of the strong vertex functions at large off shell momenta. We shall arrange the relative strength of both modifications such that e.m. vertex diagrams are still logarithmically divergent. Fortunately the pion propagator can be calculated from the pion e.m. vertex by the Ward identity, and as found in ref. [12] the model can be used to determine both quantities by an iteration procedure. Therefore no new unknown parameters enter. In principle the same could be done with the nucleon propagator, but for simplicity we shall assume that the self energy effects in both propagators are identical. There remains the question how different parametrisations of the vertex will affect predictions for the form factors, once a mass parameter in the vertex is adjusted to give the correct ρ-mass. It is clear *a priori*, that a stronger decrease in the vertex will partly be compensated by stronger self-energy contributions in the propagator.

Let us start with a discussion of the partial-wave projection of the nucleon loop of fig. 1 in the presence of vertex- and propagator-modifications. We restrict the πNN coupling to a pure pseudoscalar term and write for the vertex with nucleon momenta p_i and p_j (setting $p_i^2 - M^2 = \pi_i$ with M = nucleon mass)

$$\gamma_5 \Gamma_5(p_i, p_j) = \gamma_5 / (1 - (\pi_i + \pi_j + (p_i - p_j)^2 - \mu^2)/\Lambda_1^2) \,. \tag{2.1}$$

The cut-off parameter Λ_1^2 will be chosen to fit the ρ-mass. For the pion and nucleon propagators we take the ansatz (μ = pion mass)

$$\Delta'(p^2, \mu^2) = \frac{1}{p^2 - \mu^2} + d_2 \left(\ln \frac{p^2 - \mu^2 - 10\Lambda_2^2}{p^2 - \mu^2 - \Lambda_2^2} \right)^\delta + \sum_{i=3,4} \frac{d_i}{p^2 - \mu^2 - \Lambda_i^2}, \tag{2.2}$$

$$S'(p) = (\not{p} + M)\, \Delta'(p^2, M^2) \,. \tag{2.3}$$

The ansatz (2.3) was made for simplicity, as stated above. Simple power counting with (2.1) and (2.2) requires $\delta = \frac{1}{3}$ if the model should not be superrenormalizable. The parameters Λ_i and d_i shall be fixed [12] by adjusting (2.2) to the numerically integrated pion vertex for spacelike off-shell momenta and for $s = 0$. When we calculate the spin trace for the nucleon loop, we shall find terms proportional to π_2 and π_4. Their contribution to the $\pi\pi$ p-wave amplitude vanishes for free vertices and propagators in the loop, and we believe that they are rather small in the presence of the modifications (2.1) and (2.3) as long as $\Lambda_i^2 \gg M^2$, $i = 1, \ldots 4$. We furthermore neglect nucleon d-wave contributions, and then the p-wave projection of the loop is*

$$M_{\pi\pi}^{(1)}(k_i^2, s) \approx -\left(\frac{g^2}{4\pi}\right)^2 \frac{32}{\pi} \int_{-1}^{+1} \mathrm{d}\cos\alpha \sin\alpha \int_0^\infty \mathrm{d}q\, q^3$$

$$\times I(k_i^2, \cos\alpha, q, s)\, \Delta'(p_1^2, M^2)\, \Delta'(p_3^2, M^2)\,, \tag{2.4}$$

with

$$I(k_i^2, \cos\alpha, q, s) = (s - \pi_1 - \pi_3)\left[\tfrac{2}{3}|k_1||k_3|\, \tilde{Q}_0(k_1)\, \tilde{Q}_0(k_3)\right.$$

$$\left. + (k_1^2 + k_3^2 - 2k_{10}k_{30})\, \tilde{Q}_1(k_1)\, \tilde{Q}_1(k_3)\right] \tag{2.5}$$

$$-(k_1^2 k_4^2 + k_2^2 k_3^2 + 2\pi_1\pi_3 - (k_1^2 + k_3^2)\pi_3 - (k_2^2 + k_4^2)\pi_1)\, \tilde{Q}_1(k_1)\tilde{Q}_1(k_3).$$

We have abbreviated

$$\tilde{Q}_l(k_i) = -\frac{1}{2}\int_{-1}^{+1} \mathrm{d}z\, P_l(z)\, \Delta'((p_1 - k_i)^2, M^2)\, \Gamma_5(p_1, p_{i+1})\, \Gamma_5(p_3, p_{i+1}), \tag{2.6}$$

with $z = \cos(\boldsymbol{p}_1, \boldsymbol{k}_i)$. The loop momenta p_1 and p_3 (see fig. 1) in the c.m.s. are given by

$$P_{10(30)} = \mp\tfrac{1}{2}W - iq\cos\alpha, \qquad |\boldsymbol{p}_1| = |\boldsymbol{p}_3| = q\sin\alpha\,. \tag{2.7}$$

For pointlike vertices and free propagators the $\tilde{Q}_l(k_i)$ reduce essentially to Legendre functions of second kind. For moderately large $-k_i^2 \lesssim M^2$, the dominant term in $I(k_i^2, \cos\alpha, q, s)$ is the first one, which arises from the contraction of p_2 and p_4 in the spin trace. It consists out of an attractive, explicitely s-dependent part and the likewise attractive "contact" terms proportional to π_1 and π_3 which have little s-dependence. The relative strength of these two components of the $\pi\pi$-potential enters strongly into the ρ-width, as the s-dependent term favours a narrow, the contact terms a broad resonance.

* There is a misprint in eq. (13) of ref. [11]. The factor 2 in front of $\pi_1\pi_3$ in the formula (2.5) was omitted there, but was present in the numerical calculations.

It has been proposed by Lehmann [13] to calculate the nucleon loop with the help of the phenomenological Lagrangian due to Gursey [17]. This Lagrangian has terms like

$$L_{\pi N} = 2f_\pi^2 g_A^2 M_N : \bar{\psi}\,\psi\,\pi^2 : + \ldots , \tag{2.8}$$

which in first order just cancel the contact terms of the γ_5 interaction. Neglecting other derivative terms in the Gursey Lagrangian, the description of the p-wave phase is reasonable. But the second-order contribution of (2.8) leads to the diagram of fig. 3 for the pion f.f., which requires two subtractions. We therefore shall look for another mechanism which reduces the contact terms (anticipating the usual difficulties with the ρ-width!). Let us consider pion exchange inside the loop, fig. 4. For moderate k_i^2 we expect the leading term in the spin trace to arise again from the contraction of p_2 and p_5. At $s = k_i^2 = 0$, $i = 1, \ldots, 4$ we find from this term for the ρ-channel

$$M'^{(1)}_{\pi\pi}(s \approx k_i^2 \approx 0) = \frac{8}{3\pi}\left(\frac{g^2}{4\pi}\right)^3 \frac{|k_1||k_3|}{M^2}, \tag{2.9}$$

whereas with the same approximations one has for the simple loop

$$M^{(1)}_{\pi\pi}(s \approx k_i^2 \approx 0) = -\frac{16}{3}\left(\frac{g^2}{4\pi}\right)^2 \frac{|k_1||k_3|}{M^2}. \tag{2.10}$$

The relative factor $-g^2/8\pi^2 \approx -2.2$ between these diagrams is of course reduced by the combination of vertex and propagator modifications which will lead for off-shell momenta around $-M^2$ to an effective coupling constant g_{eff} (see sect. 5) with

$$-\frac{g_{\text{eff}}^2}{8\pi^2} \approx -\frac{1}{3}\frac{g^2}{8\pi^2} \approx -0.73 . \tag{2.11}$$

Thus a substantial part of the loop potential at $s \approx 0$ is cancelled by the repulsive one pion exchange. We think that the reduction expressed by (2.11) is too strong, since higher order contributions will reduce it. A simple calculation shows, that the linearly s-dependent term in $I(k_i^2, \cos\alpha, q, s)$ (eq. 2.5) is only weakly modified by

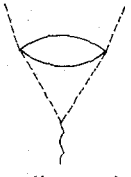

Fig. 3. Unrenormalizable pion vertex diagram due to the Lagrangian of eq. (2.8).

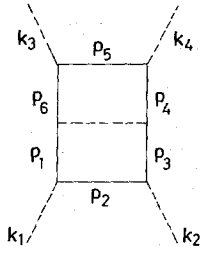

Fig. 4.

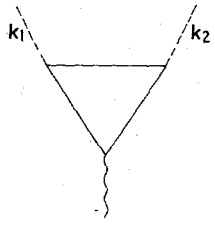

Fig. 5.

Fig. 4. Sixth-order loop diagram for the $\pi\pi$ Bethe-Salpeter kernel.

Fig. 5. Bare-nucleon current contribution to the pion e.m. form factor.

diagram fig. 4. In view of the uncertainty of any estimate like (2.9) we shall modify the contact terms in the potential by a free parameter λ, which will be used to fit the ρ-width precisely. We replace $I(k_i^2, \cos\alpha, q, s)$ by

$$I'(k_i^2, \cos\alpha, q, s) = (s - \lambda(\pi_1 + \pi_3))\,\tfrac{2}{3}|k_1||k_3|\,\tilde{Q}_0(k_1)\,\tilde{Q}_0(k_3)$$
$$+ (s - \pi_1 - \pi_3)(k_1^2 + k_3^2 - 2k_{10}k_{30})\,\tilde{Q}_1(k_1)\,\tilde{Q}_1(k_3) \qquad (2.12)$$
$$- (k_1^2 k_4^2 + k_2^2 k_3^2 + 2\pi_1\pi_3 - (k_1^2 + k_3^2)\pi_3 - (k_2^2 + k_4^2)\pi_1)\,\tilde{Q}_1(k_1)\,\tilde{Q}_1(k_3)\,.$$

It will turn out, that λ has a big influence on the high-energy behaviour of the pion f.f. We expect λ to be somewhat smaller than 1.

We now turn to the coupling of the photon to the $\pi\pi$, $K\bar{K}$ and $N\bar{N}$ state. We shall assume that there is a bare coupling of the form $e(k_1 - k_2)_\mu$ to the pion and kaon and of the form $\frac{1}{2}e\gamma_\mu$ to the isovector nucleon current. The lowest-order contribution of the nucleon current to the unrenormalized pion vertex function shown in fig. 5 is given by (using the notation 2.6):

$$F_\pi'^{(0)}(s, k_1^2, k_2^2) = 2\frac{g^2}{4\pi}\frac{1}{\pi^2}\int_{-1}^{+1} \mathrm{d}\cos\alpha\,\sin\alpha \int_0^\infty \mathrm{d}q\,q^3\,\Delta'(p_1^2, M^2)\,\Delta'(p_3^2, M^2)$$
$$\times\left((s - \lambda(\pi_1 + \pi_3))\,\tilde{Q}_0(k_1) - (s - k_1^2 - k_2^2)\frac{|q|}{|k_1|}\,\tilde{Q}_1(k_1)\right)$$
$$- 2\frac{g^2}{4\pi}\frac{1}{\pi^2} \times \text{same integral}\Big|_{s=0, k_1^2 = k_2^2 = \hat{k}^2}\,. \qquad (2.13)$$

Note the same suppression factor λ in front of the contact terms as in eq. (2.12). We regard this again as a crude approximation of diagrams with pion exchange as in

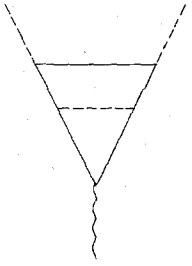

Fig. 6.

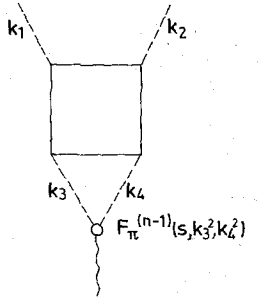

Fig. 7.

Fig. 6. Higher-order nucleon current contribution.

Fig. 7. Iterated diagram for the pion e.m. form factor.

fig. 6. The subtraction point $\hat{k}^2$ was not taken $\hat{k}^2 = \mu^2$, as this leads to a divergence of the ladder series for the pion vertex. We choose $\hat{k}^2 \approx 100\,M^2$ with the consequence that all iterated diagrams for the pion vertex are small at large momenta. We then obtained very good convergence of the ladder series. The iterated diagram with a pion current (shown in fig. 7) needs two subtractions. We write down the first subtraction for the nucleon vertex explicitly, considering a diagram with n nucleon loops (we shall denote the contributions to F_π from the nucleon current by F'_π and from the pion current by F''_π):

$$F''^{(\pi\pi,n)}_{\pi}(s, k_1^2, k_2^2) = -\frac{1}{4\pi}\frac{1}{\pi^2}\frac{1}{|k_1|}\int_{-1}^{+1} \mathrm{d}\cos\alpha \sin\alpha \int_0^\infty \mathrm{d}k\, k^3\, M^{(1)}_{\pi\pi}(k_3^2, k_4^2, k_1^2, k_2^2, s)$$

$$\times |k_3|\,\Delta'(k_3^2, \mu^2)\,\Delta'(k_4^2, \mu^2)\,F''^{(\pi\pi, n-1)}_{\pi}(s, k_3^2, k_4^2)$$

$$+ 2F'^{(0)}_{\pi}(s, k_1^2, k_2^2)\frac{4}{3}\frac{g^2}{4\pi}\frac{1}{\pi^2}\int_{-1}^{+1} \mathrm{d}\cos\alpha \sin\alpha \int_0^\infty \mathrm{d}k\, k^3 \qquad (2.14)$$

$$\times |k_3|\,\tilde{Q}_0(k_3)\,\Delta'(k_3^2, \mu^2)\,\Delta'(k_4^2, \mu^2)\,F''^{(\pi\pi, n-1)}_{\pi}(s, k_3^2, k_4^2)\Big|_{s=0, p_1^2 = p_3^2 = \hat{k}^2}$$

$$-\ \text{same expression for } s = 0,\ k_1^2 = k_2^2 = k^2,$$

with*

$$k_{30(40)} = \tfrac{1}{2}W \pm ik\cos\alpha, \qquad |k_3| = |k_4| = k\sin\alpha\,. \qquad (2.15)$$

* This representation with $-1 \leqslant \cos\alpha \leqslant +1$ is valid only for $s < 4\mu^2$.

A similar expression holds for $F_\pi'^{(\pi\pi,n)}(s, k_1^2, k_2^2)$ with $n > 0$. We shall include the kaon current everywhere by the replacement in eq. (2.14)

$$\Delta'(k_3^2, \mu^2)\,\Delta'(k_4^2, \mu^2) \to \Delta'(k_3^2, \mu^2)\,\Delta'(k_4^2, \mu^2) + \tfrac{1}{2}\Delta'(k_3^2, m_K^2)\,\Delta'(k_4^2, m_K^2)\,. \tag{2.16}$$

The final expression for the pion f.f. in the nucleon ladder approximation is now

$$\begin{aligned} F_\pi^{(\pi\pi)}(s, k_1^2, k_2^2) = {} & Z_N(\hat{k}^2) \sum_{n=0}^{\infty} F_\pi'^{(\pi\pi, n)}(s, k_1^2, k_2^2) \\ & + Z_\pi(\hat{k}^2) \sum_{n=0}^{\infty} F_\pi''^{(\pi\pi, n)}(s, k_1^2, k_2^2)\,, \end{aligned} \tag{2.17}$$

with

$$F_\pi''^{(\pi\pi, 0)}(s, k_1^2, k_2^2) = 1\,, \tag{2.18}$$

$$F_\pi'^{(\pi\pi, 0)}(s, k_1^2, k_2^2) = F_\pi'^{(0)}(s, k_1^2, k_2^2)\,, \tag{2.19}$$

as given by eq. (2.13).

The renormalization constants $Z_N(\hat{k}^2)$ and $Z_\pi(\hat{k}^2)$ could be determined separately by considering the nucleon isovector form factor simultaneously with F_π, but we simplify the model and set

$$Z_\pi(\hat{k}^2) = Z_N(\hat{k}^2)\,, \tag{2.20}$$

determined now by

$$F_\pi(0, \mu^2, \mu^2) = 1\,. \tag{2.21}$$

Other assumptions like $Z_\pi(\hat{k}^2) = 3Z_N(\hat{k}^2)$ change $F_\pi(s, \mu^2, \mu^2)$ by less than 1%. In the following we therefore shall not make any difference between $F_\pi'^{(\pi\pi, n)}$ and $F_\pi''^{(\pi\pi, n)}$ and define the renormalized contribution of n loops to the pion f.f. according to

$$F_\pi^{(n)}(s, k_1^2, k_2^2) = Z(F_\pi'^{(\pi\pi, n)}(s, k_1^2, k_2^2) + F_\pi''^{(\pi\pi, n)}(s, k_1^2, k_2^2))\,. \tag{2.22}$$

In the following sections we shall discuss the coupling of the $\pi\pi$-state and of the photon to other channels, especially to $\pi\omega$ and to $\rho\epsilon$.

3. The $\pi\omega$ channel

It has been shown in ref. [12] that the influence of the $\pi\omega$ intermediate state in the ρ-channel is rather important since it provides an attractive force which is strongly increasing with s due to the magnetic $\pi\omega\rho$ coupling. This effect reduces the ρ-width drastically. We shall derive the $\pi\pi \to \pi\omega$ amplitude again from a nucleon loop neglecting an magnetic coupling of the ω to $N\bar{N}$. Furthermore we shall assume the

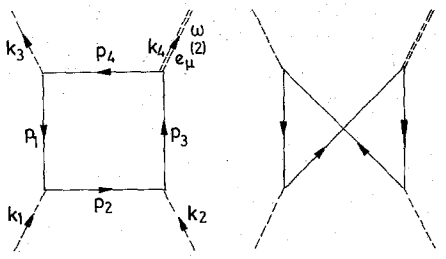

Fig. 8. (a) Nucleon-loop contribution to the $\pi\pi \to \pi\omega$ transition amplitude. (b) Crossed-nucleon loop contribution to the $\pi\pi \to \pi\omega$ transition amplitude.

same vertex correction for the $\omega N\bar{N}$ γ_μ vertex as for the $\pi N\bar{N}$ γ_5 vertex. In contrast to the $\pi\pi$ scattering case, both the uncrossed and the crossed nucleon boxes of fig. 8 contribute here. Since the crossed diagram of fig. 8b is harder to calculate than the uncrossed one, we restrict ourselves to the evaluation of fig. 8a. For small external momenta $|k_i^2| \ll M^2$, $|s| \ll M^2$ it follows from crossing symmetry that the two diagrams are identical. Since we shall treat the $\omega N\bar{N}$ coupling constant as a free parameter anyhow, this implies that we should work with an effective coupling bigger than the (unknown) physical one. From fig. 8a we get (with 2 directions for the internal momenta) for the invariant amplitude ($e_\mu(\omega)$ = polarisation vector of the ω)

$$M_{\pi\omega}^{\text{loop}}(k_i) = \frac{g^3 g_{\omega N\bar{N}}}{(4\pi)^2} \frac{4}{\pi^2} \phi_3^* \cdot (\phi_1 \times \phi_2)\, e_\mu(\omega)\, K^\mu(k_i)\,, \tag{3.1}$$

$$K_\mu(k_i) = 4iM\epsilon_{\mu\nu\rho\sigma} P^\nu k_1^\rho k_3^\sigma \int \mathrm{d}^4 q \prod_{i=1}^{4} \Gamma_5(p_i, p_{i+1})\, \Delta'(p_i^2, M^2)\,. \tag{3.2}$$

Here we have set $p_5 = p_1$ and have used the definition of $\Gamma_5(p_i, p_j)$ of (2.1). By parity conservation there is only one independent helicity amplitude of spin and isospin 1, which we take as (λ = ω-helicity)

$$M_{\pi\omega}^{(1)}(s, k_i^2) = \sqrt{\tfrac{1}{2}}(M_{\pi\omega}(s, k_i^2, \lambda = 1) - M_{\pi\omega}(s, k_i^2, \lambda = -1)) \tag{3.3a}$$

$$= -\frac{g^3 g_{\omega N\bar{N}}}{(4\pi)^2} \frac{128}{3\pi} WM |K_1| |K_3| \int_{-1}^{+1} \mathrm{d}\cos\alpha \sin\alpha \int_0^\infty \mathrm{d}\cos\alpha \sin\alpha \int_0^\infty \mathrm{d}q\, q^3$$

$$\times (\tilde{Q}_0(k_1)\, \tilde{Q}_0(k_3) - \tilde{Q}_2(k_1)\, \tilde{Q}_2(k_3))\, \Delta'(p_1^2, M^2)\, \Delta'(p_3^2, M^2)\,. \tag{3.3b}$$

This amplitude will serve as an off-diagonal kernel for the two-channel (viz. the $\pi\pi$ and the $\pi\omega$ channel) BSE.

Let us now discuss the diagonal forces in the $\pi\omega$-channel. Since the nucleon loop yields in this case many terms which are not easy to estimate, we shall concentrate on the ρ-exchange diagram fig. 9. It may be in some sense dual to the nucleon loop as ρ-exchange in $\pi\pi$ scattering was to the nucleon loop [11]. The amplitude is, following the $\rho\omega\pi$ coupling of ref. [18]:

$$M_{\omega\omega}(k_i, \lambda_2, \lambda_3) = -\frac{g^2_{\rho\omega\pi}}{4\pi}\,[e_2(\lambda_2)\cdot e_3(\lambda_3)\,(k_3\cdot k_4\, k_1\cdot k_2 - k_2\cdot k_3\, k_1\cdot k_4) + k_3\cdot e_2(\lambda_2)\, k_2\cdot e_3(\lambda_3)\, k_1\cdot k_4]\,\frac{1}{(k_1-k_3)^2 - m_\rho^2}\,. \tag{3.4}$$

The projection into the helicity state defined by (3.3a) turns out to be small compared to the $\pi\pi$-interaction, whereas the non-diagonal amplitude $M^{(1)}_{\pi\omega}$ is of the same magnitude as the latter. Thus we shall neglect the direct $\pi\omega$ interaction in the BSE.

We now turn to the description of the electromagnetic $\pi\omega$-vertex. This is, together with the $\pi^0\gamma\gamma$ vertex, traditionally explained by baryon loops [19, 20]. We calculate it from diagram fig. 10 where the blob denotes the renormalized isovector nucleon vertex. Within our approximations we have two contributions to the latter, namely the bare nucleon current denoted by (a) in fig. 11, and the full pion current denoted by (b) in fig. 11. The pion current will also contain contributions from the $\pi\omega$ intermediate states, given below in eq. (3.12). The $\pi\omega\gamma$ form factor $F_{\pi\omega\gamma}$ defined by

$$\langle \pi^0, \omega\,|j_\mu(0)|0\rangle \equiv ieF_{\pi\omega\gamma}(s, k_1^2, k_2^2)\,\epsilon_{\mu\alpha\beta\gamma}\,k_\pi^\alpha P^\beta e^\gamma(\omega)\,, \tag{3.5}$$

receives a contribution from the bare nucleon current like

$$F^{(0)}_{\pi\omega\gamma}(s, k_1^2, k_2^2) = 8Z_N(\hat{k}^2)\frac{gg_{\omega N\bar{N}}}{4\pi}\,\frac{1}{\pi^2}\,M \times \int_{-1}^{+1} \mathrm{d}\cos\theta\,\sin\theta \int_0^\infty \mathrm{d}q\, q^3\,\tilde{Q}_0(k_1)\,\Delta'(p_1^2, M^2)\,\Delta'(p_3^2, M^2)\,. \tag{3.6}$$

The f.f.s F_π and $F_{\pi\omega\gamma}$ obey now coupled BSEs which under the neglection of subtractions are written formally (suppressing integrations and constant factors)

$$F_{\pi\omega\gamma} = F^{(0)}_{\pi\omega\gamma} + M^{(1)}_{\pi\omega}(\Delta'(\mu^2)\,\Delta'(\mu^2) + 0.5\Delta'(m_K^2)\,\Delta'(m_K^2))\,F_\pi\,, \tag{3.7}$$

$$F_\pi = Z(\hat{k}^2)(1 + F'^{(0)}_\pi) + M^{(1)}_{\pi\pi}(\Delta'(\mu^2)\,\Delta'(\mu^2) + 0.5\,\Delta'(m_K^2)\,\Delta'(m_K^2))\,F_\pi + M^{(1)}_{\pi\omega}\,\Delta'(\mu^2)\,\Delta'(m_\omega^2)\,F_{\pi\omega\gamma}\,. \tag{3.8}$$

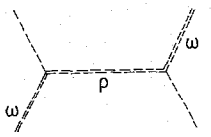

Fig. 9.

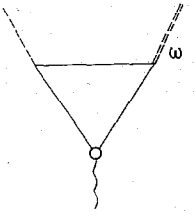

Fig. 10.

Fig. 9. ρ exchange diagram for the $\pi\omega$ scattering amplitude.

Fig. 10. Nucleon loop for the $\pi\omega\gamma$ e.m. vertex.

The coupled equations are solved by iteration.

We now exhibit the subtractions in eq. (3.7) explicity. The diagram fig. 11b involving the pion f.f. with $n-1$ loops requires a subtraction inside the loop:

$$F^{(n)}_{\pi\omega\gamma}(s, k_1^2, k_2^2) = -\frac{Z(\hat{k}^2)}{|k_1|W}\frac{1}{2\pi^3}\int_{-1}^{+1} \mathrm{d}\cos\alpha\,\sin\alpha \int_0^\infty \mathrm{d}k\,k^3\,M^{(1)}_{\pi\omega}(s, k_3^2, k_4^2, k_1^2, k_2^2)$$

$$\times |k_3|[\Delta'(k_3^2, \mu^2)\,\Delta'(k_4^2, \mu^2) + 0.5\,\Delta'(k_3^2, m_K^2)\,\Delta'(k_4^2, m_K^2)]\,F_\pi^{(n-1)}(s, k_3^2, k_4^2)$$

$$-F^{(0)}_{\pi\omega\gamma}(s, k_1^2, k_2^2)\frac{8}{3}\frac{g^2}{4\pi}\frac{1}{\pi^2}\int_{-1}^{+1} \mathrm{d}\cos\alpha\,\sin\alpha \int_0^\infty \mathrm{d}k\,k^3\,|k_3|\tilde{Q}_0(k_3) \tag{3.9}$$

$$\times [\Delta'(k_3^2, \mu^2)\,\Delta'(k_4^2, \mu^2) + 0.5\Delta'(k_3^2, m_K^2)\,\Delta'(k_4^2, m_K^2)]\,F_\pi^{(n-1)}(0, k_3^2, k_4^2)\Big|_{\substack{s=0\\ p_1^2=p_3^2=\hat{k}^2}}$$

where (3.6) has to be inserted and the kinematics of eq. (2.15) is used. Here $F_\pi^{(n)}$ is the nth iteration of eq. (3.8). We are facing a difficulty here which we cannot resolve

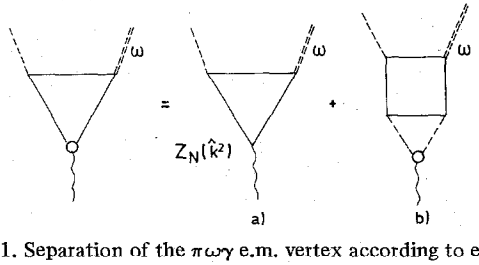

Fig. 11. Separation of the $\pi\omega\gamma$ e.m. vertex according to eq. (3.7).

at the moment. It is to be expected that with our simplifying assumption (2.18) the nucleon vertex in fig. 11 is not properly renormalized, i.e. the sum of (3.6) and (3.8) does not necessarily add up to the diagram fig. 10 with $F_1(0, M^2, M^2) = \frac{1}{2}$. On the other hand, there are other baryon loop contributions to the $\pi\omega\gamma$ vertex besides the nucleon loop, and our model cannot be too reliable here. Therefore we consider the loop of fig. 10 as an effective summation of more diagrams and do not insist on a proper normalization of $F_1(0, M^2, M^2)$. Since we are mainly interested in a realistic admixture of the $\pi\omega$ channel to the $\pi\pi$-state, we adjust $g_{\omega N\bar{N}}$ to yield [21]

$$|F_{\pi\omega\gamma}(0, \mu^2, m_\omega^2)|^2 = 3\Gamma_{\omega\to\gamma\pi}\left(\frac{2m_\omega}{m_\omega^2 - \mu^2}\right)^3 = \left(\frac{2.0 \pm 0.1}{m_\omega}\right)^2 . \tag{3.10}$$

Of course $g_{\omega N\bar{N}}$ should not deviate too much from the VDM value [22]

$$\frac{g_{\omega N\bar{N}}^2}{4\pi} = \frac{1}{4}\frac{g_\omega^2}{4\pi} = 4.6 \pm 0.5 . \tag{3.11}$$

Since we neglected a direct $\pi\omega \to \pi\omega$ amplitude, the $\pi\omega$ intermediate state contributes only internally in the pion f.f. in fig. 11b. The contribution of the $\pi\omega$ intermediate states to $F_\pi(s, k_1^2, k_2^2)$ is without subtractions (see fig. 12 and the last term of eq. (3.8)) given by

$$F_\pi^{(\pi,\omega)}(s, k_1^2, k_2^2) = \frac{W}{|\boldsymbol{k}_1|}\frac{1}{4\pi^3}\int_{-1}^{+1} \mathrm{d}\cos\alpha \, \sin\alpha \int_0^\infty \mathrm{d}k \, k^3$$

$$\times M_{\pi\omega}^{(1)}(s, k_3^2, k_4^2, k_1^2, k_2^2)\, \Delta'(k_3^2, \mu^2)\, \Delta'(k_4^2, m_\omega^2)\, F_{\pi\omega\gamma}(s, k_3^2, k_4^2) .$$

This term vanishes like s for $s \to 0$.

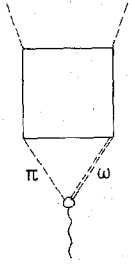

Fig. 12. Contribution of the $\pi\omega$ intermediate state to the pion e.m. form factor.

4. The $\rho\epsilon$ loop as a long range force in the $\pi\pi$ channel

Due to our general idea that non-diagonal forces are dominant in the π-π channel we consider the exchange of two pions via $\rho\epsilon$ intermediate states as the leading long range force contribution in the ρ-channel. The total $\rho\epsilon$ loop contribution to the invariant $\pi\pi$ amplitude of fourth order is given by the two s-channel box diagrams of fig. 2a and the two u-channel box diagrams of fig. 2b. Unfortunately, the u-channel box contribution cannot be evaluated in analogy to the nucleon box calculations, as it involves four-particle intermediate states in the s-channel. Therefore, these diagrams (and also those of the s-channel box) are evaluated by use of dispersion relations in t for fixed s. The s-channel box amplitude has only a "right-hand" cut given by the two pion intermediate states, whereas the u-channel box has also a "left-hand" cut given by the $\rho\epsilon$ intermediate states. This method of calculating the diagrams, however, is only applicable in the energy range where the anomalous singularities of the triangle diagram, obtained by contracting one of the ρ or ϵ propagators, are not on the physical sheet [23]. The corresponding condition is e.g. $k_1^2 + k_3^2 \leqslant 2(m_\rho^2 + \mu^2)$. The most disadvantageous case is that k_2 and k_4 are on their mass shell, which arises from picking up the propagator poles in the Wick-rotated Bethe-Salpeter equation above threshold. Then we have $(\sqrt{s} - \mu)^2 \leqslant m_\rho^2 + \mu^2$, which is an upper energy bound for the applicability of our method.

Throughout our calculation we put $m_\rho = m_\epsilon = m$. The sum of the two diagrams of fig. 2a and the two diagrams of fig. 2b gives the invariant amplitude

$$M_{\rho\epsilon}(k_i) = -i \frac{g_{\rho\pi\pi}^2}{4\pi} \frac{g_{\epsilon\pi\pi}^2}{4\pi} \frac{m^2}{\pi^2} \int \mathrm{d}^4 q \left[\frac{I^{(s)} R^{(s)}(k_i, q)}{\prod_{i=1}^{4} (p_i^2 - m_i^2)} + \frac{I^{(u)} R^{(u)}(k_i, q)}{\prod_{i=1}^{4} (p_i'^2 - m_i^2)} \right], \tag{4.1}$$

where $m_1 = m_3 = m$ and $m_2 = m_4 = \mu$.

$I^{(s)}$ and $I^{(u)}$ are the isospin factors of the s-channel boxes and u-channel boxes, respectively, i.e. $I^{(s)} = 2$, $I^{(u)} = 1$. The coupling constants $g_{\rho\pi\pi}$ and $g_{\epsilon\pi\pi}$ are related to the total widths of $\rho \to \pi\pi$ and $\epsilon \to \pi\pi$ by

$$\frac{g_{\rho\pi\pi}^2}{4\pi} = \tfrac{3}{2} m_\rho^2 \frac{\Gamma_{\rho\pi\pi}}{(\frac{1}{4} m_\rho^2 - \mu^2)^{\frac{3}{2}}}, \qquad \frac{g_{\epsilon\pi\pi}^2}{4\pi} = \frac{4}{3} \frac{\Gamma_{\epsilon\pi\pi}}{\sqrt{\frac{1}{4} m_\epsilon^2 - \mu^2}}. \tag{4.2}$$

The spin terms $R^{(s)}(k_i, q)$ and $R^{(u)}(k_i, q)$ are defined according to

$$\begin{aligned} R^{(s)}(k_i, q) &= R_1(k_i) + 8 |\boldsymbol{k}_1| |\boldsymbol{k}_3| \cos\theta_{13} + \pi_1 + \pi_3 \\ &\quad + R_2(k_3, k_4)\pi_2 + R_2(k_1, k_2)\pi_4 + \frac{1}{m^2}\pi_2\pi_4, \end{aligned} \tag{4.3}$$

$$R^{(u)}(k_i, q) = R_1(k_i) + 8|k_1||k_3|\cos\theta_{13} + \pi_1' + \pi_3' + R_2(k_2, k_3)\pi_2' + R_2(k_1, k_4)\pi_4' + \frac{1}{m^2}\pi_2'\pi_4', \tag{4.4}$$

where R_1 and R_2 are functions of the external momenta

$$R_1(k_i) = k_1^2 + k_2^2 + k_3^2 + k_4^2 - 4k_{10}k_{30} - 4k_{20}k_{40} - 4\mu^2 + 2m^2 + \frac{1}{m^2}(\mu^2 - k_1^2)(\mu^2 - k_3^2) + \frac{1}{m^2}(\mu^2 - k_2^2)(\mu^2 - k_4^2), \tag{4.5}$$

$$R_2(k_j, k_l) = \frac{1}{m^2}(2\mu^2 - 2m^2 - k_j^2 - k_l^2), \tag{4.6}$$

and π_i is the abbreviation $\pi_i = p_i^2 - m_i^2$ ($\pi_i' = p_i'^2 - m_i^2$). For the s-channel box contribution the terms which are proportional to π_2 and π_4 can be dropped because they only contribute to s-waves. For the u-channel box contribution, however, only the term proportional to $\pi_2' \cdot \pi_4'$ can be dropped. $M_{\rho e}(k_i)$ is evaluated by writing down a dispersion relation in t for fixed s with a "right-hand" cut contribution and a "left-hand" cut contribution. We obtain the expression

$$\begin{aligned} M_{\rho e}(k_i) = \frac{g_{\rho\pi\pi}^2}{4\pi}\frac{g_{e\pi\pi}^2}{4\pi}\,2m^2 \Bigg\{ & \int_{4\mu^2}^{\infty} \mathrm{d}t' \,\frac{1}{t'-t}\,\frac{\sqrt{\frac{1}{4}t'-\mu^2}}{2\sqrt{t'}} \\ & \times [(R_1(k_i) + 8|k_1||k_3|\cos\theta_{13})(2K_{13}^{(+)}(t') + K_{13}^{(-)}(t')) \\ & + 2K_1^{(+)}(t') + 2K_3^{(+)}(t') + K_1^{(-)}(t') + K_3^{(-)}(t')] \\ & + \int_{4m^2}^{\infty} \mathrm{d}u' \,\frac{1}{u'-u}\,\frac{\sqrt{\frac{1}{4}u'-m^2}}{2\sqrt{u'}} [(R_1(k_i) + 8|k_1||k_3|\cos\theta_{13})K_{24}^{(-)}(u') \\ & + R_2(k_2, k_3)K_4^{(-)}(u') + R_2(k_1, k_4)K_2^{(-)}(u')] \Bigg\}, \end{aligned} \tag{4.7}$$

where $K_i^{(\pm)}$ and $K_{ij}^{(\pm)}$ are defined according to

$$K_i^{(+)} = \frac{1}{2\pi}\int \mathrm{d}\Omega_q \frac{1}{\pi_i}, \quad K_{ij}^{(+)} = \frac{1}{2\pi}\int \mathrm{d}\Omega_q \frac{1}{\pi_i\pi_j},$$
$$K_i^{(-)} = \frac{1}{2\pi}\int \mathrm{d}\Omega_q \frac{1}{\pi_i'}, \quad K_{ij}^{(-)} = \frac{1}{2\pi}\int \mathrm{d}\Omega_q \frac{1}{\pi_i'\pi_j'}. \tag{4.8}$$

The integrals occurring in the "right-hand" cut contribution are evaluated in the t-channel c.m.s. with the momenta p_2 and p_4 kept on their mass-shell, whereas the integrals occurring in the "left-hand" cut contribution are evaluated in the u-channel c.m.s. with the momenta p_1 and p_3 kept on their mass shell. With the t-channel kinematics

$$p_{20} = \tfrac{1}{2}\sqrt{t}, \quad |\boldsymbol{p}_2| = \sqrt{\tfrac{1}{4}t - \mu^2}, \quad |\boldsymbol{k}_i| = \sqrt{k_{i0}^2 - k_i^2},$$
$$k_{10} = \frac{1}{2\sqrt{t}}(t + k_1^2 - k_3^2), \quad k_{20} = \frac{1}{2\sqrt{t}}(k_4^2 - k_2^2 - t), \tag{4.9}$$

and the cosines

$$z_1 = \frac{m^2 - \mu^2 - k_1^2 + 2p_{20}k_{10}}{2|\boldsymbol{p}_2||\boldsymbol{k}_1|}, \qquad z_2 = \frac{\mu^2 + k_2^2 - m^2 + 2p_{20}k_{20}}{2|\boldsymbol{p}_2||\boldsymbol{k}_2|},$$
$$z_{12} = \frac{k_1^2 + k_2^2 - s + 2k_{10}k_{20}}{2|\boldsymbol{k}_1||\boldsymbol{k}_2|}, \tag{4.10}$$

one obtains the explicit form

$$K_1^{(+)}(t) = K_1^{(-)}(t) = \frac{1}{2|\boldsymbol{k}_1||\boldsymbol{p}_2|} \ln\frac{z_1 - 1}{z_1 + 1}, \tag{4.11}$$

$$K_3^{(+)}(t) = K_3^{(-)}(t) = \frac{1}{2|\boldsymbol{k}_2||\boldsymbol{p}_2|} \ln\frac{1 + z_2}{z_2 - 1}, \tag{4.12}$$

$$K_{13}^{(\pm)}(t) = \frac{1}{4|\boldsymbol{k}_1||\boldsymbol{k}_2||\boldsymbol{p}_2|^2} \frac{1}{D_\pm} \ln\frac{(a_\pm + b_\pm - D_\pm)(b_\pm + D_\pm)}{(a_\pm + b_\pm + D_\pm)(b_\pm - D_\pm)}, \tag{4.13}$$

where

$$a_\pm = (z_1 + z_2)^2 - 2(1 \pm z_{12}), \qquad b_\pm = -z_2(z_1 + z_2) + 1 \pm z_{12},$$
$$c = z_2^2 - 1, \qquad D_\pm = \sqrt{b_\pm^2 - ca_\pm}. \tag{4.14}$$

Similarly with the u-channel kinematics

$$p'_{30} = \tfrac{1}{2}\sqrt{u}, \qquad |\boldsymbol{p}'_3| = \sqrt{\tfrac{1}{4}u - m^2}, \qquad |\boldsymbol{k}_i| = \sqrt{k_{i0}^2 - k_i^2},$$
$$k_{20} = \frac{1}{2\sqrt{u}}(k_3^2 - k_2^2 - u), \qquad k_{40} = \frac{1}{2\sqrt{u}}(k_1^2 - k_4^2 - u), \tag{4.15}$$

and the cosines

$$v_2 = \frac{m^2 + k_2^2 - \mu^2 + 2p'_{30}k_{20}}{2|\boldsymbol{p}'_3||\boldsymbol{k}_2|}, \qquad v_4 = \frac{m^2 + k_4^2 + 2p_{30}k_{40} - \mu^2}{2|\boldsymbol{p}'_3||\boldsymbol{k}_4|},$$
$$v_{24} = \frac{k_1^2 + k_3^2 - s - u + 2k_{20}k_{40}}{2|\boldsymbol{k}_2||\boldsymbol{k}_4|}, \tag{4.16}$$

one finds the result

$$K_2^{(-)}(u) = \frac{1}{2|\boldsymbol{p}'_3||\boldsymbol{k}_2|} \ln\frac{v_2+1}{v_2-1}, \qquad K_4^{(-)}(u) = \frac{1}{2|\boldsymbol{p}'_3||\boldsymbol{k}_4|} \ln\frac{v_4+1}{v_4-1}, \tag{4.17}$$

$$K_{24}^{(-)}(u) = \frac{1}{4|\boldsymbol{k}_2||\boldsymbol{k}_4||\boldsymbol{p}'_3|^2} \frac{1}{D} \ln\frac{(a+b-D)(b+D)}{(a+b+D)(b-D)}, \tag{4.18}$$

with

$$a = (v_2 - v_4)^2 - 2(1 - v_{24}), \qquad b = (v_2 - v_4)v_4 + 1 - v_{24},$$
$$c = v_4^2 - 1, \qquad D = \sqrt{b^2 - ac}. \tag{4.19}$$

Performing the $J = 1$ projection of eq. (4.7) we finally obtain

$$M_{\rho\epsilon}^{(1)}(k_i) = \frac{g_{\epsilon\pi\pi}^2}{4\pi} \frac{g_{\rho\pi\pi}^2}{4\pi} \frac{m^2}{|\boldsymbol{k}_1||\boldsymbol{k}_3|} \Bigg\{ \int_{4\mu^2}^{\infty} \mathrm{d}t' \frac{\sqrt{\frac{1}{4}t' - \mu^2}}{2\sqrt{t'}}$$
$$\times \left[(R_1(k_i)(2K_{13}^{(+)}(t') + K_{13}^{(-)}(t')) + 3K_1^{(+)}(t') + 3K_3^{(+)}(t')) Q_1(w_{t'}) \right.$$
$$\left. + \tfrac{8}{3}|\boldsymbol{k}_1||\boldsymbol{k}_3|(2K_{13}^{(+)}(t') + K_{13}^{(-)}(t'))(Q_0(w_{t'}) + 2Q_2(w_{t'})) \right] \tag{4.20}$$
$$- \int_{4m^2}^{\infty} \mathrm{d}u' \frac{\sqrt{\frac{1}{4}u' - m^2}}{2\sqrt{u'}} \left[(R_1(k_i)K_{24}^{(-)}(u') + R_2(k_2, k_3)K_4^{(-)}(u') + R_2(k_1, k_4)K_2^{(-)}(u'))Q_1(w_{u'}) \right.$$
$$\left. + \tfrac{8}{3}|\boldsymbol{k}_1||\boldsymbol{k}_3|K_{24}^{(-)}(u')(Q_0(w_{u'}) + 2Q_2(w_{u'})) \right] \Bigg\},$$

where $w_{t'}$ and $w_{u'}$ are defined according to

$$w_{t'} = \frac{1}{2|\boldsymbol{k}_1||\boldsymbol{k}_3|}(2k_{10}k_{30} + t' - k_1^2 - k_3^2), \qquad w_{u'} = \frac{1}{2|\boldsymbol{k}_1||\boldsymbol{k}_3|}(2k_{10}k_{30} + k_2^2 + k_4^2 - s - u'). \tag{4.21}$$

As input in our Bethe-Salpeter kernel we use eq. (4.20) with the vertex modifications

$$\frac{g^2_{\epsilon\pi\pi}}{4\pi}\frac{g^2_{\rho\pi\pi}}{4\pi} \to \frac{g^2_{\epsilon\pi\pi}}{4\pi}\frac{g^2_{\rho\pi\pi}}{4\pi}\prod_{j=1}^{4}\left(1-\frac{k_j^2}{M^2}\right)^{-1}. \tag{4.22}$$

These modifications due to the resonance wave functions are justified from our model for the ρ, and we speculate that the $\epsilon\pi\pi$ vertex is similar to the $\rho\pi\pi$ vertex. As we are interested in the long range character of the $\rho\epsilon$-loop we do not consider propagator modifications of the exchanged pions and use vertex functions which are independent of the internal momenta.

We shall assume that the $\rho\epsilon$-loop diagrams are coupled to the photon via the dressed pion propagators and the renormalized pion vertex as shown in fig. 13. Due to the vertex corrections (4.22) the diagrams fig. 13 are finite and do not need an internal subtraction, but they have to be subtracted nevertheless for $k_1^2 = k_2^2 = k^2$. Thus we obtain for the $\rho\epsilon$-contribution to the unrenormalized pion form factor with n nucleon or $\rho\epsilon$-loops

$$\begin{aligned} F_\pi^{(\rho\epsilon,n)}(s,k_1^2,k_2^2) = &-\frac{1}{4\pi^3}\frac{1}{|k|}\int_{-1}^{+1}\mathrm{d}\cos\alpha\sin\alpha\int_0^\infty \mathrm{d}q\,q^3 \\ &\times M^{(1)}_{\rho\epsilon}(s,k_3^2,k_4^2,k_1^2,k_2^2)\prod_{j=1}^{4}\left(1-\frac{k_j^2}{M^2}\right)^{-1} \\ &\times |k_3|\,\Delta'(k_3^2,\mu^2)\,\Delta'(k_4^2,\mu^2)\,F_\pi^{(n-1)}(s;k_3^2,k_4^2) \\ &- \text{same expression}\Big|_{s=0,\,k_1^2=k_2^2=\hat{k}^2}. \end{aligned} \tag{4.23}$$

Here $F^{(n-1)}$ is the $(n-1)$th iteration of eq. (3.8) with the substitution

$$M^{(1)}_{\pi\pi} \to M^{(1)}_{\pi\pi} + M^{(1)}_{\rho\epsilon}. \tag{4.24}$$

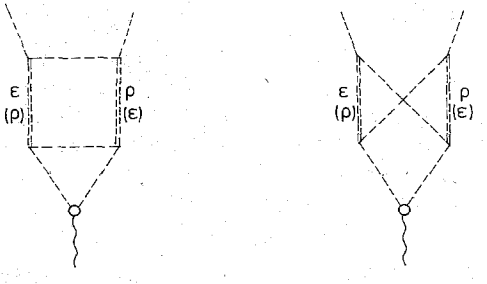

Fig. 13. Contributions of the $\rho\epsilon$ intermediate state to the pion c.m. form factor.

5. Numerical results

We have solved the coupled integral equations (3.7) and (3.8) by numerical iteration and subsequent "Padéisation" of the Born series for $F_\pi(s) \equiv F_\pi(s, \mu^2, \mu^2)$. Due to the mentioned limitations in s for the dispersion representation of the $\rho\epsilon$ box diagram, we have restricted the calculation to the interval

$$-m_\rho^2 \leqslant s \leqslant m_\rho^2 . \tag{5.1}$$

There we have calculated $F_\pi(s)$ at 10 roughly equally spaced points s_i $(i = 1, ..., 10)$ with a relative accuracy of the order of 10^{-5}. We have extrapolated $F_\pi(s)$ to values of s outside this region, following a suggestion of ref. [24], with a generalized effective range expansion

$$F_\pi(s) = \frac{\sum_{n=0}^{N_a} a_n k_\pi^{2n} + \sum_{n=1}^{N_b} b_n k_\pi^{2n+1} f(k_\pi) + c k_\omega^3 f(k_\omega)}{\sum_{n=0}^{N'_a} a'_n k_\pi^{2n} + \sum_{n=1}^{N'_b} b'_n k_\pi^{2n+1} f(k_\pi) + c' k_\omega^3 f(k_\omega)} , \tag{5.2}$$

with

$$k_\pi = \sqrt{\tfrac{1}{4}s - \mu^2}, \qquad k_\omega = \sqrt{s - (m+\mu)^2} ,$$

$$f(k) = \ln((W + 2k)/(W - 2k))/W , \tag{5.3}$$

$$a'_0 = 1 .$$

The coefficients a_0 to c' are determined by a least square fit of (5.2) to the 14 "data" points $F_\pi(s_i)$ $(i = 1, ..., 10)$, including Im $F_\pi(s)$. The extrapolation is stable within 10% for $|F_\pi(s)|^2$ in the range $s < 3$ GeV^2. The details of this method will be published elsewhere.

In the following we shall discuss three dynamically different versions. First of all we neglect the $\rho\epsilon$ loop and work only with the coupled $\pi\pi$ and $\pi\omega$ channels. The width of the ρ-meson is adjusted through the parameter λ in eq. (2.12). This is version A. In order to illustrate the effect of other inelastic channels on the form factor, we speculatively add a short range $\rho\epsilon$ contribution in the same way and strength as the $\bar{K}K$-contribution in eq. (3.8). In this version B we need a somewhat larger value λ than in A. Finally in version C we include the $\rho\epsilon$ loop, keeping also the short range part of version B. We now shall present the results for the $\pi\pi$ p-wave phase shift, the e.m. pion vertex $F_\pi(0, q^2, q^2)$ and for $F_\pi(s)$ both in the spacelike and timelike region for the versions A, B and C.

Version A. The values of the cut-off parameter Λ_1^2 and the propagator parameters d_2, Λ_2^2 etc., for λ and for $g^2_{\omega N\bar{N}}/4\pi$ are given in table 1. The resulting value

Table 1
Values of the hadronic cut-off mass Λ_1^2, the suppression factor λ, the propagator parameters $d_2 \ldots \Lambda_4^2$, the coupling constant $g_{\omega N\bar{N}}$, the vertex constant $|F_{\pi\omega\gamma}|$ and the $\pi\pi$ p-wave scattering length in the three different versions A, B and C explained in sect. 5.

	Λ_1^2 (M^2)	λ	d_2	Λ_2^2 (M^2)	d_3	Λ_3^2 (M^2)	d_4	Λ_4^2 (M^2)	$\frac{g^2_{\omega N\bar{N}}}{4\pi}$	$\lvert F_{\pi\omega\gamma}\rvert$ (m_ω^{-1})	a_1^1 (μ^{-2})
A	2.55	0.61	0.0043	2.72	4.0	88.5	0	0	19.9	1.93	0.021
B	2.39	0.66	0.0043	2.72	4.0	88.5	0	0	19.9	1.87	0.023
C	2.11	0.65	0.0045	2.72	6.8	99.5	0.1	1.1	21.1	1.77	0.048

for $F_{\pi\omega\gamma}(0, \mu^2, m_\omega^2)$ is shown in the same table. As expected, we need a $\omega N\bar{N}$ coupling constant larger than the VDM value (3.11) by about a factor 2 for adjusting $F_{\pi\omega\gamma}$, due to the omission of the crossed nucleon box fig. 8b. In fig. 14 we show the vertex function $F_\pi(0. k^2, k^2)$ for spacelike k^2, together with the ratio

$$R_\Delta(k^2) = \frac{\Delta(k^2)}{\Delta'(k^2)}. \tag{5.4}$$

This ratio agrees with the integrated form of the Ward identity

$$\Delta(k^2) \int_{\mu^2}^{k^2} \mathrm{d}k'^2 F_\pi(0, k'^2, k'^2) = R_\Delta(k^2) \tag{5.5}$$

within 2%. It is reassuring, that $F_\pi(0, k^2, k^2)$ does not differ drastically from the hadronic vertex (2.1) with $\Lambda_1^2 = 2.55\, M^2$, which allows vaguely a consistent picture for all vertices.

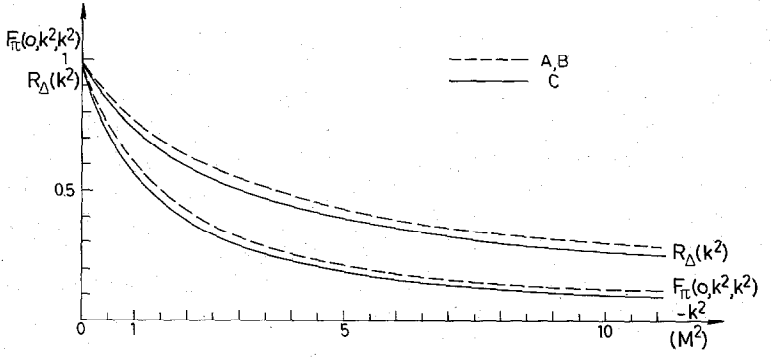

Fig. 14. E.M. pion vertex function $F_\pi(0, k^2, k^2)$ and ratio $R(k^2) = \Delta(k^2)/\Delta'(k^2)$ of free to renormalized pion propagator, for versions A, B and C.

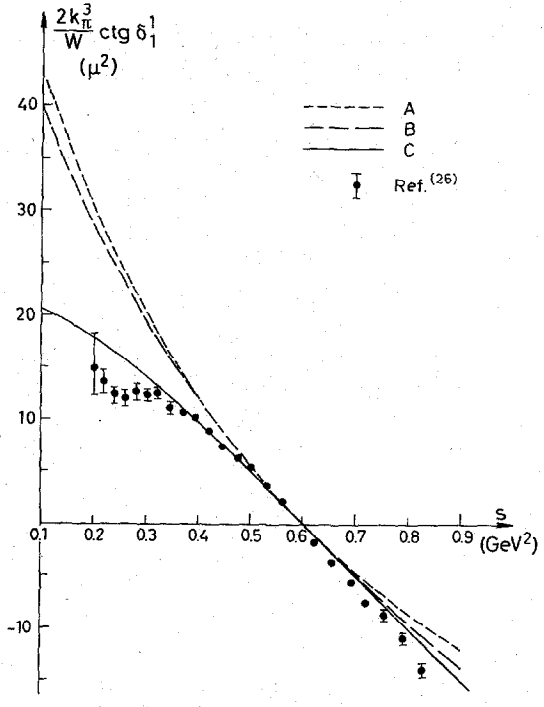

Fig. 15. $\pi\pi$ phase shift $\delta_1^1(s)$ for versions A, B and C. Data are from ref. [26].

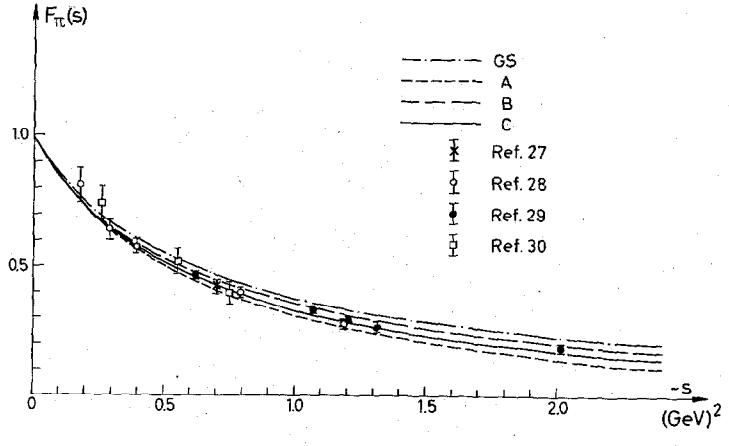

Fig. 16. E.M. pion f.f. $F_\pi(s)$ in the space-like region for versions A, B and C. GS denotes the Gounaris-Sakurai formula refs. [9,10].

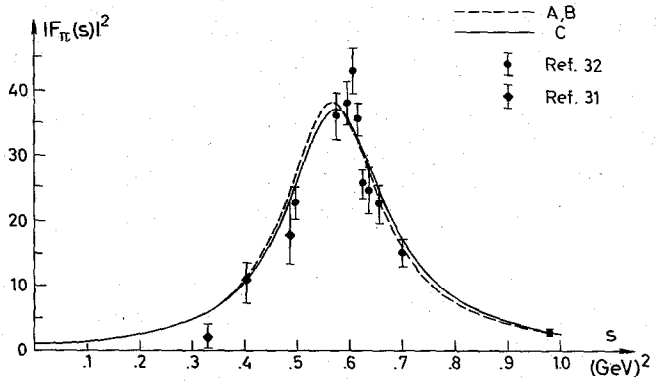

Fig. 17. Same as fig. 16 in the ρ region.

Since at least up to the $\pi\omega$ threshold (and possibly somewhat above) we have

$$\arg F_\pi(s) = \arg t_{\pi\pi}^{I=J=1}(s) \equiv \delta_1^1(s)\,, \tag{5.6}$$

we can extract $\delta_1^1(s)$ from our calculation. We show the effective range plot in fig. 15. It extrapolates to a scattering length

$$a_1^1(A) = 0.021\,\mu^{-2}\,, \tag{5.7}$$

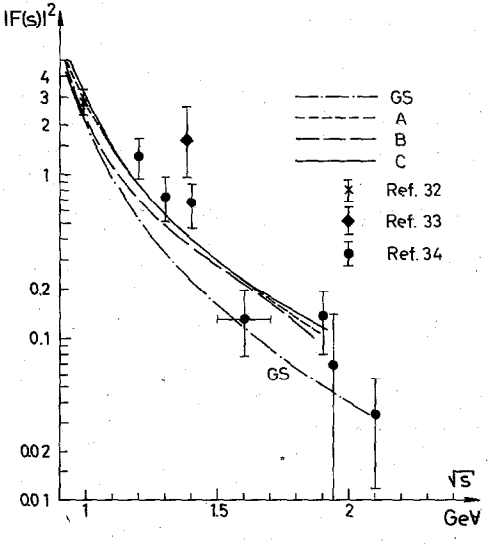

Fig. 18. Same as fig. 16 above the ρ region.

somewhat low compared to the current algebra value [25] $a_1 = 0.03\mu^{-2}$. The phase shift does not agree well with that extracted [26] from the CERN-Munic experiment at 17.2 GeV.

In figs. 16–18 we compare the resulting pion f.f. with the available data [27–34] in the space-like region, resonance region and large time-like region. There is a slight tendency for a too strong decrease in the space-like region (fig. 16). The reverse will be true in version B, to which we shall turn now.

Version B. The inclusion of another inelastic channel will of course reduce the ρ-mass and width with all other parameters kept constant. We therefore have to decrease Λ_1^2 and increase λ to retain the correct ρ properties, as seen in table 1. The effects on the vertex function and on $F_{\pi\omega\gamma}$ are small. The phase shift $\delta_1^1(s)$ changes slightly such that the effective range curve fig. 15 has less curvature in the wrong direction. One obtains

$$a_1^1(\mathrm{B}) = 0.023\mu^{-2} . \tag{5.8}$$

The deviations from the Gounaris-Sakurai curve in the space-like region (fig. 16) are now smaller than in version A, which is due to the increase in the parameter λ. The same is true in the large s time-like region (fig. 18).

Version C. We have now included the $\rho\epsilon$ loop calculated with

$$\frac{g_{\rho\pi\pi}^2}{4\pi}\,\frac{g_{\epsilon\pi\pi}^2}{4\pi} = 3.74 , \tag{5.9}$$

which leads with $g_{\rho\pi\pi}^2/4\pi = 2.5$ to a value $\Gamma_{\epsilon\pi\pi} = 360$ MeV. This value is somewhat low compared with the value of $\geqslant 600$ MeV in ref. [21], but on the other hand it leads to a s-wave scattering length somewhat larger than that extrapolated from the reaction [26] $\pi^- \mathrm{p} \to \pi^+\pi^- \mathrm{n}$. The effective range curve now obtains a definite downward curvature in agreement with experiment (see fig. 15). One finds

$$a_1^1(C) = 0.048\mu^{-2} . \tag{5.10}$$

Since the long range component of the ρ-vertex function is enhanced by the pion exchange contribution, the vertex function $F_\pi(0, q^2, q^2)$ in fig. 14 drops faster than in version A with a corresponding downward shift in $R_\Delta(q^2)$. With the hadronic vertex function (2.1) and the resulting $R_\Delta(q^2)$ we can define an effective coupling constant $g_{\mathrm{eff}}(k^2)$ by

$$g_{\mathrm{eff}}^2(k^2) = g^2 R_\Delta^{-3}(k^2 - M^2)\left(1 - 3\frac{(k^2 - M^2)}{\Lambda_1^2}\right)^{-2} . \tag{5.11}$$

Here all three-momenta of the vertex are taken equally far from the mass shell, which is reasonable at low energies. We obtain in version C

$$g^2_{\text{eff}}(-M^2) = 0.32\, g^2 \,, \tag{5.12}$$

which has been used in sect. 2. For large negative $k^2 g^2_{\text{eff}}(k^2)$ converges to $0.25\, g^2$. The resulting pion f.f. is shown by a full line in figs. 16–18. It agrees well with the data in all three regions of s. The small shift of the peak position in the resonance region compared to version A is a consequence of the difference in the $\pi\pi$ phase shift at low energies.

6. Conclusions

We have presented a model for the e.m. form factor of the pion which contains as unknown (or badly known) parameters a hadronic cut-off mass, a suppression factor for contact terms in the nucleon loop and the coupling constants $g_{\omega N\bar{N}}$ and $g_{\epsilon\pi\pi}$. Furthermore we tentatively have added a short-range $\pi\pi \to \rho\epsilon$ coupling which has to be calculated from a contact term. The first two parameters are fixed by the ρ-mass and width whereas $g_{\omega N\bar{N}}$ is determined by $F_{\pi\omega\gamma}$, and $g_{\epsilon\pi\pi}$ rather poorly by $\Gamma_{\epsilon\pi\pi}$. A more consistent determination of $g_{\epsilon\pi\pi}$ and of the short range $\pi\pi \to \rho\epsilon$ part may be possible by considering the process $\gamma \to \rho\epsilon$ in the same model. It is an advantage of this model that all parameters, except λ, are of a general nature, i.e. they appear in many other amplitudes or form factors. Since λ is well determined by Γ_ρ, we are close to a parameter free description of $F_\pi(s)$. We think that the model contains many important aspects of strong interactions, namely the presence of both long range (of order μ^{-1}) and short range (of order M^{-1}) forces, strong damping in vertex functions and increase in propagators and finally the coupling of many channels already at moderate energies. It is an essential improvement over a Bethe-Salpeter model proposed previously [35]. Future aspects on the theoretical side are the following: The higher-order corrections in the nucleon loop should be calculated more carefully not only because of the energy behaviour of the $\pi\pi$ potential, but also because of current conservation requirements. Both the use of dressed nucleon propagators and of damped meson nucleon vertices requires the inclusion of diagrams of the general form fig. 6. Strong violations of current conservation might ultimately destroy the possibility to renormalize the pion and nucleon form factors as in eq. (2.17) with positive renormalization constants Z_π and Z_N. Our results for the pion f.f. show significant deviations from a pure ρ-dominance expression [10], however without higher vector mesons or strong cups as proposed by Renard [4]. The present experiments [32–34] support such deviations, but are inconclusive with respect to sizeable effects of various ρ' or cusps. If such effects show up in further experiments, our model needs essential modifications.

One of us (U.W.) wishes to thank Professors H. Joos, H. Schopper and G. Weber for the kind hospitality extended to him at DESY.

References

[1] Y. Oyanagi, Prog. Theor. Phys. 42 (1969) 898.
[2] N.G. Antoniou, C.G. Georgalas and C.B. Uouris, Nuovo Cimento Letters 4 (1970) 915.
[3] M. Böhm and M. Krammer, Phys. Letters 50B (1974) 457.
[4] F.M. Renard, Phys. Letters 47B (1973) 361.
[5] V.N. Baier and V.S. Fadin, Pisma JETP (Sov. Phys.) 15 (1972) 219.
[6] M. Roos, preprint Univ. Helsinki nr. 63 (1973).
[7] B.R. Webber, Phys. Rev. D3 (1971) 1971.
[8] R. Omnès, Nuovo Cimento 8 (1958) 316.
[9] W. Frazer and J. Fulco, Phys. Rev. Letters 2 (1959) 365.
[10] G.J. Gounaris and J.J. Sakurai, Phys. Rev. Letters 21 (1968) 244.
[11] F. Gutbrod, Phys. Rev. D6 (1972) 3631.
[12] F. Gutbrod, DESY 72/74.
[13] H. Lehmann, DESY 72/54 (1972); Recent developments in mathematical physics, ed. Paul Urban (Springer, Wien, 1973).
[14] G. Ecker and J. Honerkamp, Nucl. Phys. B62 (1973) 509.
[15] V.N. Pervushin and M.K. Volkov, Dubna JINR E2-7661 (1974).
[16] J. Zinn-Justin, Phys. Reports 1 (3) (1971).
[17] F. Gürsey, Nuovo Cimento 16 (1960) 230.
[18] M. Gell-Man, D. Sharp and W.G. Wagner, Phys. Rev. Letters 8 (1962) 261.
[19] J. Steinberger, Phys. Rev. 76 (1949) 1180.
[20] M.D. Scadron and R.L. Thews, Phys. Rev. D6 (1972) 844.
[21] Particle Data Group, Rev. Mod. Phys. 45 (1973) 1.
[22] J. Le Francois, Proc. of the Int. Symp. on electron and photon interactions at high energies, 1971, ed. by N.B. Mistry (Cornell Univ. Press, Ithaca, 1972).
[23] R.J. Eden, P.V. Landshoff, D.I. Olive and J.C. Polkinghorne, The analytic S-matrix (Cambridge University Press, 1966).
[24] R.W. Haymaker and L. Schlessinger, The Padé approximant in theoretical physics, ed. G.A. Baker and J.L. Gammel (Academic Press, New York, 1970) p. 257.
[25] S. Weinberg, Phys. Rev. Letters 17 (1966) 168.
[26] P. Estabrooks et al., AIP Proc. of the Int. Conf. on $\pi\pi$ scattering and associated topics, Tallahassee, Florida, 1973, p. 37.
[27] P.S. Kummer et al., Nuovo Cimento Letters 1 (1971) 1026.
[28] C.N. Brown et al., Phys. Rev. D8 (1973) 92.
[29] C.J. Bebek et al., Phys. Rev. D9 (1974) 1229.
[30] C. Driver et al., Phys. Letters 35B (1971) 77, 81;
F. Gutbrod and G. Kramer, Nucl. Phys. B49 (1972) 461.
[31] V.L. Auslander et al., Sov. J. Nucl. Phys. 9 (1969) 69.
[32] D. Benaksas et al., Phys. Letters 39B (1972) 289.
[33] V.E. Balakin et al., Phys. Letters 41B (1972) 205.
[34] M. Bernardini et al., Phys. Letters 46B (1973) 261.
[35] J. Fleischer and F. Gutbrod, Nuovo Cimento 10A (1972) 235.